Journal of Structural Chemistry. Vol. 52, No. 1, pp. 151-159, 2011

$Ru_2(CO)_4\{OOC(CH_2)_nCH_3\}_2L_2$ SAWHORSE-TYPE COMPLEXES CONTAINING μ_2-η^2-CARBOXYLATO LIGANDS DERIVED FROM SATURATED FATTY ACIDS

© **J. P. Johnpeter and B. Therrien** UDC 548.736:546.96:547.12

The thermal reaction of $Ru_3(CO)_{12}$ with the saturated fatty acids (heptanoic, nonanoic, decanoic, tridecanoic, tetradecanoic, heptadecanoic, octadecanoic) in refluxing tetrahydrofuran, followed by addition of triphenylphosphine (PPh_3) or pyridine (C_5H_5N), gives the dinuclear complexes $Ru_2(CO)_4\{OOC(CH_2)_nCH_3\}_2L_2$ (**1**: $n = 5$, **2**: $n = 7$, **3**: $n = 8$, **4**: $n = 11$, **5**: $n = 12$, **6**: $n = 15$, **7**: $n = 16$; **a**: L = NC_5H_5, **b**: L = PPh_3). The single crystal structure analysis of **1b**, **2a**, **3a**, **4a** and **5a** reveals a dinuclear $Ru_2(CO)_4$ sawhorse structure, the diruthenium backbone being bridged by the carboxylato ligands, while the two L ligands occupy the axial positions at the ruthenium atoms. In **2a**, π–π stacking interactions between adjacent pyridyl units of symmetry related molecules prevail, while in the longer alkyl chain derivatives **3a**, **4a** and **5a**, additional van der Waals and electrostatic interactions between the alkyl chains take place as well in the packing arrangement of the molecules, thus giving rise to layers of parallel alkyl chains in the crystal.

Keywords: carbonyl ligands, carboxylato bridges, fatty acids, dinuclear complexes, ruthenium.

INTRODUCTION

Sawhorse-type ruthenium complexes of the type $Ru_2(CO)_4(OOCR)_2L_2$, L being a two-electron donor ligand, are well-known since 1969, when J. Lewis and co-workers reported their formation by refluxing $Ru_3(CO)_{12}$ in various carboxylic acids followed by depolymerisation of the obtained materials in coordinating solvents [1]. These dinuclear complexes were shown later, by a single-crystal X-ray structure analysis of $Ru_2(CO)_4(OOCBu^n)_2(PBu^t_3)_2$, to possess a $Ru_2(CO)_4$ backbone in a sawhorse-type arrangement with two μ_2-η^2-carboxylato bridges ($OOCBu^n$) and two axial two-electron donor ligands (PBu^t_3) [2]. Since their discovery, a considerable number of such sawhorse-type diruthenium complexes with carboxylato bridges have been synthesised and they have been studied in different field of applications [3].

Herein, we report the synthesis, characterisation and molecular structure of fourteen new $Ru_2(CO)_4$ sawhorse-type complexes containing carboxylato ligands derived from saturated fatty acids. The single-crystal structure analysis of five representative complexes is presented as well.

Institut de Chimie, Université de Neuchâtel, 51 Ave de Bellevaux, CH-2000 Neuchâtel, Switzerland; bruno.therrien@unine.ch. The text was submitted by the authors in English. *Zhurnal Strukturnoi Khimii*, Vol. 52, No. 1, pp. 155-163, January-February, 2011. Original article submitted March 26, 2010.

RESULTS AND DISCUSSION

Dodecacarbonyltriruthenium reacts with the appropriate carboxylic acid (heptanoic, nonanoic, decanoic, tridecanoic, tetradecanoic, heptadecanoic, octadecanoic) in refluxing tetrahydrofuran to give, in the presence of triphenylphosphine or pyridine (L), the dinuclear complexes $Ru_2(CO)_4\{OOC(CH_2)_nCH_3\}_2L_2$ in reasonable yields, see Scheme 1.

$$2/3Ru_3(CO)_{12} + 2CH_3(CH_2)_nCOOH + 2L \rightarrow Ru_2(CO)_4\{OOC(CH_2)_nCH_3\}_2L_2 + 4CO + 2H_2$$

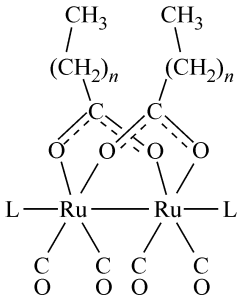

L	$n = 5$	$n = 7$	$n = 8$	$n = 11$	$n = 12$	$n = 15$	$n = 16$
NC_5H_5	**1a**	**2a**	**3a**	**4a**	**5a**	**6a**	**7a**
PPh_3	**1b**	**2b**	**3b**	**4b**	**5b**	**6b**	**7b**

Scheme 1. Synthesis of the dinuclear complexes $Ru_2(CO)_4\{OOC(CH_2)_nCH_3\}_2L_2$ (**1**-**7**).

All compounds are air-stable yellow crystalline powders which have been characterised by their infrared, NMR and mass spectrometry as well as by their micro-analytical data. All compounds exhibit in the $\nu_{(CO)}$ region of the infrared spectrum the characteristic pattern of the $Ru_2(CO)_4$ sawhorse unit, which consist of three bands (very-strong; medium; very-strong) between 2100 cm^{-1} and 1900 cm^{-1} [3]. The triphenylphosphine derivatives **1b**–**7b** show in their ^{31}P NMR spectra ($CDCl_3$, 23°C) a singlet at ≈15 ppm, typical of a triphenylphosphine ligand being coordinated to a $Ru_2(CO)_4(O_2CCR)_2$ dinuclear core [4-6].

The single-crystal structure analysis of **1b** shows as expected a $Ru_2(CO)_4$ sawhorse backbone with the two triphenylphosphine ligands in the axial positions and the carboxylato bridges in the equatorial positions, see Fig. 1. The Ru–Ru distance (2.7239(5) Å) is in the range of a ruthenium-ruthenium single bond, as it was also observed in analogous complexes containing triphenylphosphine axial ligands [4-6]. The P–Ru–Ru–P torsion angle is 40.4(2)°, which is comparable to those observed in $Ru_2(CO)_4\{O_2CCH_2O–C_6H_2Cl_2–COC(CH_2)C_2H_5\}_2(PPh_3)_2$ [4] and $Ru_2(CO)_4(O_2CC_5H_4FeC_5H_5)_2(PPh_3)_2$ [6].

Similarly, the single-crystal structure analyses of **2a**, **3a**, **4a**, and **5a** exhibit the $Ru_2(CO)_4$ sawhorse backbone with the two pyridyl ligands in the axial positions and the carboxylato bridges in the equatorial positions (Fig. 2). Selected geometrical parameters are given in Table 1. The Ru–Ru distances (**2a**: 2.6804(8) Å, **3a**: 2.6817(5) Å, **4a**: 2.6793(14) Å, **5a**: 2.6829(5) Å) are as well in the range of a ruthenium-ruthenium single bond but they are considerably shorter than the one observed in the triphenylphosphine derivative **1b** (Table 1). This difference in the metal–metal distance can be associated to an increase in electron density between the metal atoms as a result of the lack of back-bonding to the pyridyl ligands.

In the crystal packing of **2a**, closed parallel π–π stacking interactions is observed between pyridyl groups of two adjacent dinuclear complexes (Fig. 3). The centroid-centroid separation is 3.73 Å and agreed well with the theoretical value calculated for this π stacking mode [7].

Similarly, in the crystal packing of **3a**, **4a**, and **5a**, parallel π stacking interactions are observed between neighbouring pyridyl moieties of adjacent sawhorse complexes, however, the centroid-centroid separations are slightly shorter in these crystals (**3a**: 3.64 Å, **4a**: 3.63 Å, **5a**: 3.64 Å). The presence of longer alkyl chains in **3a**, **4a** and **5a** induces

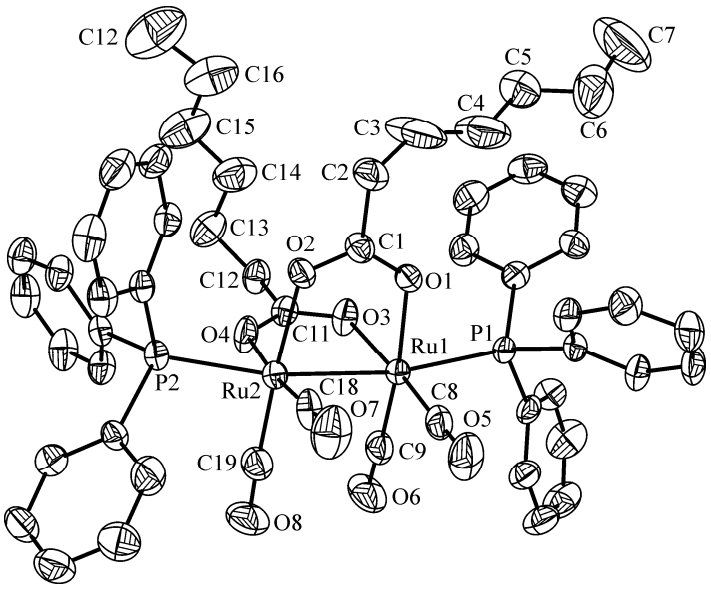

Fig. 1. ORTEP drawing of $Ru_2(CO)_4\{OOC(CH_2)_5CH_3\}_2(PPh_3)_2$ (**1b**) at 50% probability level ellipsoids with hydrogen atoms omitted for clarity.

TABLE 1. Selected Bond Lengths (Å) and Angles (deg) for **1b**, **2a**, **3a**, **4a**, and **5a**

Parameter	**1b**	**2a**	**3a**	**4a**	**5a**
			Distances (Å)		
Ru–Ru	2.7239(5)	2.6804(8)	2.6817(5)	2.6793(14)	2.6829(5)
$Ru–P_{PPh3}$	2.4566(11)				
$Ru–P_{PPh3}$	2.4296(11)				
$Ru–N_{pyridine}$		2.223(6)	2.224(3)	2.246(9)	2.215(4)
$Ru–N_{pyridine}$		2.211(6)	2.209(3)	2.206(9)	2.216(4)
$Ru–O_{carboxylato}$	2.123(3)	2.128(6)	2.148(3)	2.122(8)	2.150(3)
$Ru–O_{carboxylato}$	2.114(3)	2.120(5)	2.115(3)	2.123(8)	2.118(3)
$Ru–O_{carboxylato}$	2.138(3)	2.131(6)	2.126(3)	2.136(8)	2.125(4)
$Ru–O_{carboxylato}$	2.114(3)	2.124(6)	2.127(3)	2.132(8)	2.121(4)
			Angles (deg)		
$O_{carboxylato}$					
O–Ru–O	85.06(14)	83.3(2)	82.81(12)	81.4(4)	82.82(15)
O–Ru–O	84.32(12)	83.7(2)	83.22(12)	82.3(3)	83.47(16)
$C_{carbonyl}$					
C–Ru–C	90.2(2)	88.5(4)	88.3(2)	86.7(6)	88.3(2)
C–Ru–C	88.4(2)	89.4(4)	89.3(2)	88.4(5)	89.4(2)
			Torsion angles (deg)		
L–Ru–Ru–L	40.4(2)	–6.5(11)	10.2(5)	–6.1(16)	9.0(6)

a different packing arrangement as compared to **2a**. Indeed, to maximise van der Waals and electrostatic interactions between alkyl chains, and to optimise packing density, the two alkyl chains of the sawhorse complex adopt a parallel arrangement. Moreover, these parallel pair of alkyl chains interacts with neighbouring parallel pairs of alkyl chains from symmetry related molecules to generate layers of alkyl chains. As an example, the head-to-tail arrangement of parallel alkyl chains observed in

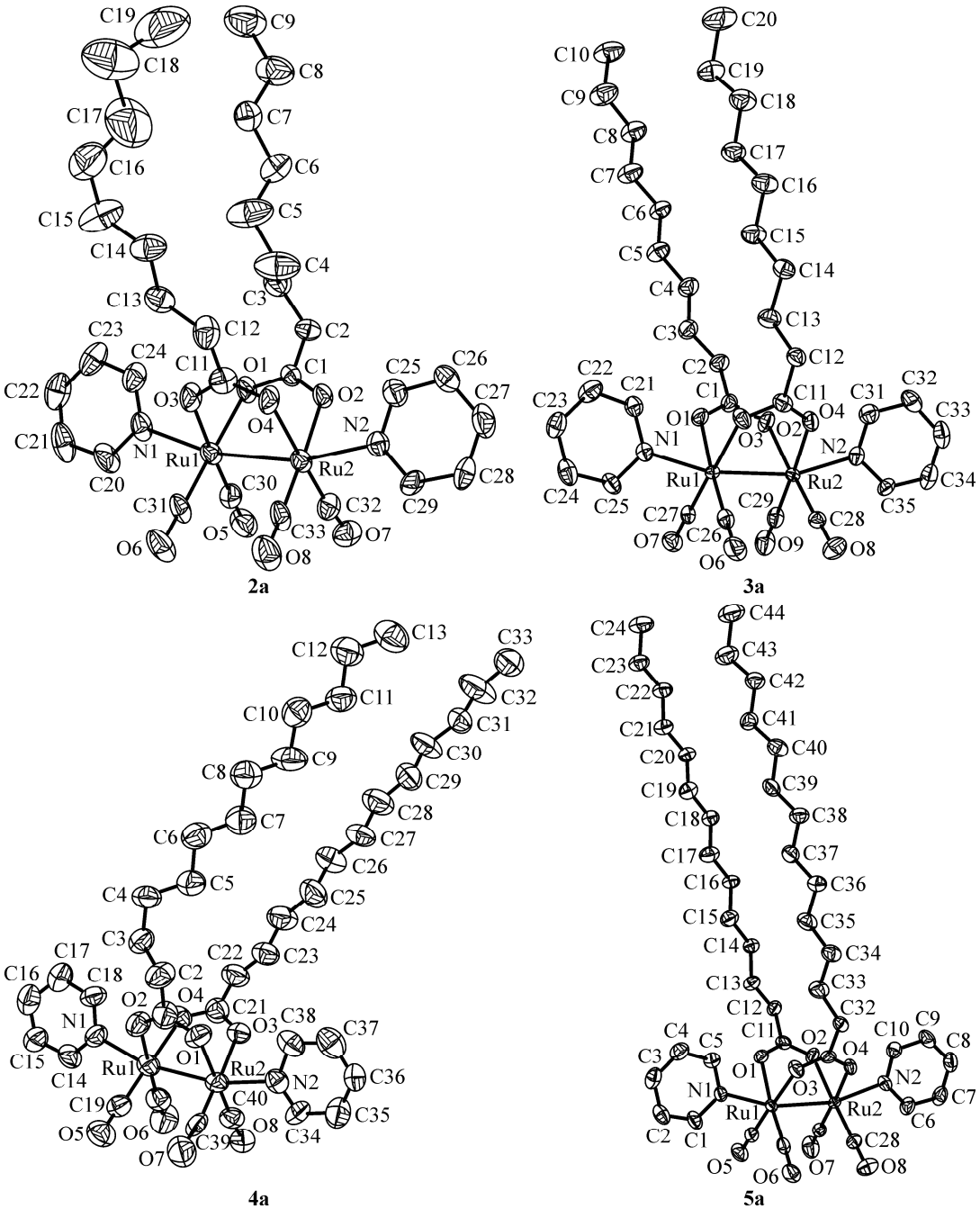

Fig. 2. ORTEP drawings of $Ru_2(CO)_4\{OOC(CH_2)_7CH_3\}_2(C_5H_5N)_2$ (**2a**), $Ru_2(CO)_4\{OOC(CH_2)_8CH_3\}_2(C_5H_5N)_2$ (**3a**), $Ru_2(CO)_4\{OOC(CH_2)_{11}CH_3\}_2(C_5H_5N)_2$ (**4a**) and $Ru_2(CO)_4\{OOC(CH_2)_{12}CH_3\}_2(C_5H_5N)_2$ (**5a**) at 50% probability level ellipsoids with hydrogen atoms omitted for clarity.

5a is presented in Fig. 4. The width of these layers is approximately 14.0 Å in **3a** [Ru–Ru separation], while in **4a** it reaches 17.6 Å and in **5a** it is greater than 25.0 Å.

In conclusion, we have synthesised and characterised fourteen new sawhorse-type complexes containing various *n*-alkyl carboxylato bridging ligands. The single-crystal structure analyses of five representatives reveal that for $n \geq 8$, the packing of the alkyl chains and the π–π interactions between pyridyl groups dominate, while for $n \leq 7$, only the arrangement of the axial pyridyl ligands plays a significant role in the crystalline packing of these sawhorse-type complexes derived from saturated fatty acids.

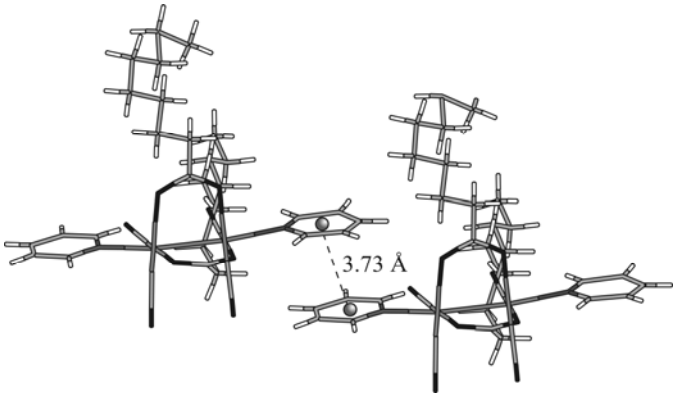

Fig. 3. Parallel π stacking interaction observed in the crystalline packing of **2a**.

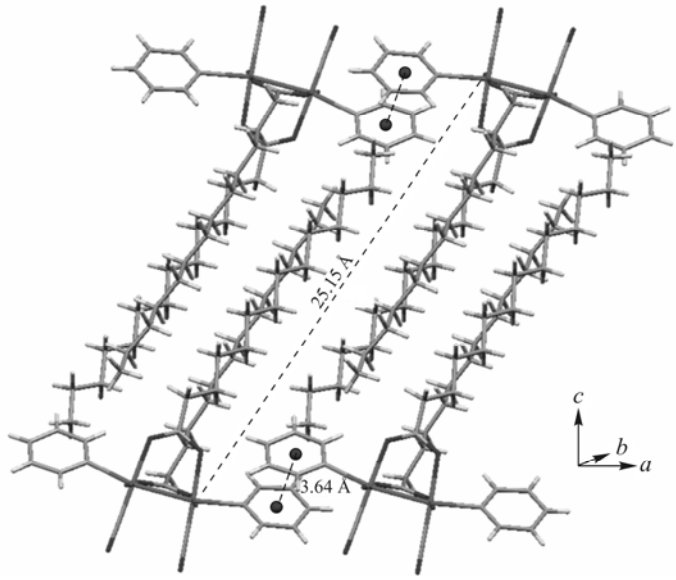

Fig. 4. Main interactions involved in the crystalline packing of **5a**, π stacking interactions between adjacent pyridyl groups and van der Waals interactions between parallel alkyl chains.

EXPERIMENTAL

General. All manipulations were carried out by routine under nitrogen atmosphere. Organic solvents were degassed and saturated with nitrogen prior to use. All fatty acids were purchased either from Aldrich or Fluka and used as received. Dodecacarbonyltriruthenium was prepared according to published methods [8]. NMR spectra were recorded on a Bruker AvanceII 400 MHz spectrometer. IR spectra were recorded on a Perkin-Elmer 1720X FT-IR spectrometer (4000-400 cm^{-1}). Microanalyses were performed by the Laboratory of Pharmaceutical Chemistry, University of Geneva (Switzerland). Electro-spray mass spectra were obtained in positive-ion mode with a Bruker FTMS 4.7 T BioAPEX II mass spectrometer.

General method for the preparation of complexes 1-7. A solution of $Ru_3(CO)_{12}$ (100 mg, 0.16 mmol) and the appropriate carboxylic acid (0.47 mmol) in dry tetrahydrofuran (25 ml) was heated at 120°C in a pressure Schlenk tube for 22 h. Then the appropriate axial ligand L (0.47 mmol) was added (L = pyridine **1a-7a**, L = triphenylphosphine **1b-7b**). The solution was stirred at room temperature for 3 hours, evaporated and the product isolated from the residue by crystallisation from a tetrahydrofuran/hexane or dichloromethane/pentane mixture. In order to improve the purity, the raw product was

subjected to thin-layer chromatography on silica gel using dichloromethane/pentane as eluents and obtained as yellow products.

$Ru_2(CO)_4\{OOC(CH_2)_5CH_3\}_2(C_5H_5N)_2$ (**1a**). Yellow powder, yield 50 mg (43.74%). ^{1}H NMR (400 MHz, $CDCl_3$): δ = 8.73-8.75 (m, 4H, C_5H_5N), 7.81-7.85 (*tt*, 2H, C_5H_5N, ^3J = 7.6Hz, ^4J = 1.6 Hz), 7.44-7.48 (m, 4H, C_5H_5N), 2.27 (*t*, 4H, CH_2COO, ^3J = 7.3 Hz), 1.22-1.24 (m, 20H, CH_2), 0.85 (*t*, 6H, CH_3, ^3J = 6.8 Hz). $^{13}C\{^1H\}$ NMR (100 MHz, $CDCl_3$) δ = 205.13 (CO), 195.70 (CO), 183.90 (COO), 151.83 (C_5H_5N), 36.86 (CH_2), 31.83 (CH_2), 29.41 (CH_2), 29.18 (CH_2), 26.62 (CH_2), 14.05 (CH_3). IR (KBr): $\nu_{(CO)}$ 2021 vs, 1966 m, 1945 m, $\nu_{(OCO)}$ 1568 s cm^{-1}. ESI-MS: *m*/*z* = 674.30 $[M\text{-}2CO]^+$. Anal. Calc. for $C_{54}H_{50}N_2O_8Ru_2$: C, 45.95; H, 4.87. Found C, 46.02; H, 4.97%.

$Ru_2(CO)_4\{OOC(CH_2)_5CH_3\}_2(PPh_3)_2$ (**1b**). Yellow crystalline solid, yield 161 mg (93.87%). ^{1}H NMR (400 MHz, $CDCl_3$): δ = 7.55-7.39 (m, 30H, CH_{ph}), 1.94 (*t*, 4H, CH_2COO, ^3J = 7.3 Hz), 0.91-1.40 (m, 16H, CH_2), 0.84 (*t*, 6H, CH_3, ^3J = 7.2 Hz). $^{13}C\{^1H\}$ NMR (100 MHz, $CDCl_3$): δ = 205.13 (CO), 195.70 (CO), 183.90 (COO), 133.87 (CH_{ph}), 133.81 (CH_{ph}), 133.75 (CH_{ph}), 133.40 (CH_{ph}), 129.52 (CH_{ph}), 128.03 (CH_{ph}), 127.99 (CH_{ph}), 37.15 (CH_2), 31.52 (CH_2), 28.77 (CH_2), 25.67 (CH_2), 22.47 (CH_2), 22.64 (CH_2), 14.04 (CH_3). $^{31}P\{^1H\}$ NMR (161 MHz, ($CDCl_3$): δ = 14.21 ppm. IR (KBr): $\nu_{(CO)}$ 2024 vs, 1977 m, 1951 m, $\nu_{(OCO)}$ 1565 s cm^{-1}. ESI-MS: *m*/*z* = 1015.72 $[M\text{-}3CO]^+$. Anal. Calc. for $C_{54}H_{50}O_8P_2Ru_2$: C, 59.02; H, 4.97. Found C, 59.12; H, 5.14%.

$Ru_2(CO)_4\{OOC(CH_2)_7CH_3\}_2(C_5H_5N)_2$ (**2a**). Yellow crystalline solid, yield 80 mg (65.04%). ^{1}H NMR (400 MHz, $CDCl_3$): δ = 8.75-8.73 (m, 4H, C_5H_5N), 7.81-7.85 (*tt*, 2H, C_5H_5N, ^3J = 7.6Hz, ^4J = 1.6 Hz), 7.40-7.43 (m, 4H, C_5H_5N), 2.27 (*t*, 4H, CH_2COO, ^3J = 7.3 Hz), 1.22-1.28 (m, 20H, CH_2), 0.87 (*t*, 6H, CH_3, ^3J = 6.9 Hz). $^{13}C\{^1H\}$ NMR (100 MHz, CDCl3): δ = 151.83 (C_5H_5N), 137.19 (C_5H_5N), 124.69 (C_5H_5N), 36.86 (CH_2), 31.83 (CH_2), 29.41 (CH_2), 29.18 (CH_2), 26.62 (CH_2), 14.05 (CH_3). IR (KBr): $\nu_{(CO)}$ 2021 vs, 1968 m, 1945 m, $\nu_{(OCO)}$ 1567 s cm^{-1}. ESI-MS: *m*/*z* = 758.76 $[M\text{-}CO+H]^+$. Anal. Calc. for $C_{58}H_{64}N_2O_8Ru_2$: C, 48.76; H, 5.66; N, 3.50. Found C, 48.89; H, 5.64; N, 3.56%.

$Ru_2(CO)_4\{OOC(CH_2)_7CH_3\}_2(PPh_3)_2$ (**2b**). Yellow crystalline solid, yield 50 mg (27.70%). ^{1}H NMR (400 MHz, $CDCl_3$): δ = 7.55-7.39 (m, 30H, CH_{ph}), 1.94 (*t*, 4H, CH_2COO, ^3J = 7.3 Hz), 1.44-0.90 (m, 24H, CH_2), 0.87 (*t*, 6H, CH_3, ^3J = 7.1Hz). $^{13}C\{^1H\}$ NMR (100 MHz, $CDCl_3$): δ = 205.85 (CO), 188.37 (COO), 151.06 (CO), 133.87 (CH_{ph}), 133.81 (CH_{ph}), 133.75 (CH_{ph}), 133.25 (CH_{ph}), 133.40 (CH_{ph}), 133.25 (CH_{ph}), 37.16 (CH_2), 31.86 (CH_2), 29.33 (CH_2), 29.18 (CH_2), 29.13 (CH_2), 25.74 (CH_2), 22.64 (CH_2), 14.07 (CH_3). $^{31}P\{^1H\}$ NMR (161 MHz, $CDCl_3$): δ = 14.22 ppm. IR (KBr): $\nu_{(CO)}$ 2019 vs, 1974 m, 1942 m, $\nu_{(OCO)}$ 1559 s cm^{-1}. ESI-MS: *m*/*z* = 1070.72 $[M\text{-}3CO]^+$. Anal. Calc. for $C_{64}H_{58}O_8P_2Ru_2$: C, 60.41; H, 5.59. Found C, 60.55; H, 5.66%.

$Ru_2(CO)_4\{OOC(CH_2)_8CH_3\}_2(C_5H_5N)_2$ (**3a**). Yellow crystalline solid, yield 80 mg (32.00%). ^{1}H NMR (400 MHz, $CDCl_3$): δ = 8.75-8.73 (m, 4H, C_5H_5N), 7.85-7.81 (m, 2H, C_5H_5N), 7.43-7.40 (m, 4H, C_5H_5N), 2.27 (*t*, 4H, CH_2COO,^3J = 7.1 Hz), 1.22-1.28 (m, 20H, CH_2), 0.88 (*t*, 6H, CH_3, ^3J = 6.9 Hz). $^{13}C\{^1H\}$ NMR (100 MHz, $CDCl_3$): δ = 151.83 (C_5H_5N), 137.09 (C_5H_5N), 124.09 (C_5H_5N), 36.86(CH_2), 31.83(CH_2), 29.41(CH_2), 29.18(CH_2), 26.62 (CH_2), 14.05 (CH_3). IR (KBr): $\nu_{(CO)}$ 2021 vs, 1966 m, 1945 m, $\nu_{(OCO)}$ 1568 s cm^{-1}. ESI-MS: *m*/*z* = 759.10 $[M\text{-}2CO]^+$. Anal. Calc. for $C_{34}H_{68}N_2O_8Ru_2$: C, 49.12; H, 5.82; N, 3.29. Found C, 50.11; H, 5.94; N, 3.44%.

$Ru_2(CO)_4\{OOC(CH_2)_8CH_3\}_2(PPh_3)_2$ (**3b**). Yellow powder, yield 127 mg (69.03%). ^{1}H NMR (400 MHz, $CDCl_3$): δ = 7.55-7.26 (m, 30H, CH_{ph}), 1.97 (*t*, 4H, CH_2COO, ^3J = 7.2 Hz), 1.25–0.90 (m, 28H, CH_2), 0.92 (*t*, 6H, CH_3, ^3J = 7Hz). $^{13}C\{^1H\}$ NMR (100 MHz, $CDCl_3$): δ = 205.48 (CO), 205.44 (CO), 205.40 (CO), 188.49 (COO), 188.34 (COO), 133.91 (CH_{ph}), 133.85 (CH_{ph}), 133.79 (CH_{ph}), 133.58 (CH_{ph}), 133.42 (CH_{ph}), 133.27 (CH_{ph}), 37.21 (CH_2), 31.93 (CH_2), 29.54 (CH_2), 29.44 (CH_2), 25.79 (CH_2), 22.70 (CH_2), 14.16 (CH_3). $^{31}P\{^1H\}$ NMR (161 MHz, ($CDCl_3$): δ = 14.01 ppm. IR (KBr): $\nu_{(CO)}$ 2018 vs, 1976 m, 1942 m, $\nu_{(OCO)}$ 1557 s cm^{-1}. ESI-MS: *m*/*z* = 1180.35$[M+H]^+$. Anal. Calc. for $C_{60}H_{68}O_8P_2Ru_2$: C, 61.01; H, 5.80. Found C, 59.98; H, 5.71%.

$Ru_2(CO)_4\{OOC(CH_2)_{11}CH_3\}_2(C_5H_5N)_2$ (**4a**). Yellow crystalline solid, yield 85 mg (55.19%). ^{1}H NMR (400 MHz, $CDCl_3$): δ = 8.75-8.73 (m, 4H, C_5H_5N), 7.85-7.81 (m, 2H, C_5H_5N), 7.43-7.40 (m, 4H, C_5H_5N), 2.26 (*t*, 4H, CH_2COO,

^3J = 7.1 Hz), 1.25-1.22 (m, 48H, CH_2), 0.88 (*t*, 6H, CH_3, ^3J = 7.2 Hz). $^{13}C\{^1H\}$ NMR (100 MHz, $CDCl_3$): δ = 206.13 (CO), 195.42 (CO), 183.91 (COO), 151.83 (C_5H_5N), 36.96 (CH_2), 31.84 (CH_2), 29.30 (CH_2), 29.18 (CH_2), 26.26 (CH_2), 14.36 (CH_3). IR (KBr): $\nu_{(CO)}$ 2022 vs, 1968 m, 1945 m, $\nu_{(OCO)}$ 1569 s cm^{-1}. ESI-MS: *m*/*z* = 843.19 $[M\text{-}2CO]^+$. Anal. Calc. for $C_{40}H_{60}N_2O_8Ru_2$: C, 53.17; H, 6.53; N, 2.99. Found C, 53.44; H, 6.72; N, 3.11%.

$Ru_2(CO)_4\{OOC(CH_2)_{11}CH_3\}_2(PPh_3)_2$ (**4b**). Yellow powder, yield 85 mg (42.92%). ^1H NMR (400 MHz, $CDCl_3$): δ = 7.58-7.26 (m, 30H, CH_{ph}), 1.94 (*t*, 4H, CH_2COO, ^3J = 7.2 Hz), 1.28-1.01 (m, 40H, CH_2), 0.90 (*t*, 6H, CH_3, ^3J = 6.8 Hz). $^{13}C\{^1H\}$ NMR (100 MHz, $CDCl_3$): δ = 205.48 (CO), 205.46 (CO), 205.42 (CO), 205.38 (CO), 188.47 (COO), 188.39 (COO), 188.39 (COO), 133.89 (CH_{ph}), 133.77 (CH_{ph}), 133.56 (CH_{ph}), 133.40 (CH_{ph}), 133.25 (CH_{ph}), 129.54 (CH_{ph}), 37.18 (CH_2), 31.92 (CH_2), 29.77 (CH_2), 29.58 (CH_2), 25.43 (CH_2), 22.69 (CH_2), 14.13 (CH_3). $^{31}P\{^1H\}$ NMR: (161 MHz, ($CDCl_3$): δ = 14.23 ppm. IR (KBr): $\nu_{(CO)}$ 2021 vs, 1974 m, 1943 m, $\nu_{(OCO)}$ 1558 s cm^{-1}. ESI-MS: *m*/*z* = 1266.35 $[M+H]^+$. Anal. Calc. for $C_{66}H_{80}O_8P_2Ru_2$: C, 62.64; H, 6.37. Found C, 62.73; H, 6.51%.

$Ru_2(CO)_4\{OOC(CH_2)_{12}CH_3\}_2(C_5H_5N)_2$ (**5a**). Yellow crystalline solid, yield 50 mg (34.48%). ^1H NMR (400 MHz, $CDCl_3$): δ = 8.75-8.73 (m, 4H, C_5H_5N), 7.84-7.80 (m, 2H, C_5H_5N), 7.43-7.40 (m, 4H, C_5H_5N), 2.28 (*t*, 4H, CH_2COO, ^3J = 7.2 Hz), 1.26-1.22 (m, 48H, CH_2), 0.88 (*t*, 6H, CH_3, ^3J = 6.8 Hz). $^{13}C\{^1H\}$ NMR (100 MHz, $CDCl_3$): δ = 204.10 (CO), 186.94 (COO), 151.84 (C_5H_5N), 137.22 (C_5H_5N), 124.72 (C_5H_5N), 36.87 (CH_2), 31.89 (CH_2), 29.68 (CH_2), 29.64 (CH_2), 29.58 (CH_2), 29.51 (CH_2), 29.41 (CH_2), 29.34 (CH_2), 29.20 (CH_2), 29.04 (CH_2), 26.19 (CH_2), 24.70 (CH_2), 22.65 (CH_2), 14.08 (CH_3). IR (KBr): $\nu_{(CO)}$ 2022 vs, 1969 m, 1944 m, $\nu_{(OCO)}$ 1568 s cm^{-1}. ESI-MS: *m*/*z* = 872.22 $[M\text{-}2CO]^+$. Anal. Calc. for $C_{42}H_{64}N_2O_8Ru_2$: C, 54.03; H, 6.92; N, 2.91. Found C, 54.41; H, 6.99; N, 3.02%.

$Ru_2(CO)_4\{OOC(CH_2)_{12}CH_3\}_2(PPh_3)_2$ (**5b**). Yellow powder, yield 60 mg (30.28%). ^1H NMR (400 MHz, $CDCl_3$): δ = 7.52-7.35 (m, 30H, CH_{ph}), 1.91 (*t*, 4H, CH_2COO, ^3J = 7.2 Hz), 1.65-0.90 (m, 44H, CH_2), 0.88 (*t*, 6H, CH_3, ^3J = 6.8 Hz). $^{13}C\{^1H\}$ NMR (100 MHz, $CDCl_3$): δ = 205.85 (CO), 188.37 (COO), 151.06 (CO), 133.87 (CH_{ph}), 133.81 (CH_{ph}), 133.75 (CH_{ph}), 133.40 (CH_{ph}), 129.51 (CH_{ph}), 128.08 (CH_{ph}), 37.16 (CH_2), 31.89 (CH_2), 29.63 (CH_2), 29.56 (CH_2), 29.33 (CH_2), 25.74 (CH_2), 22.65 (CH_2), 14.08 (CH_3). $^{31}P\{^1H\}$ NMR (161 MHz, $CDCl_3$): δ = 14.21 ppm. IR (KBr): $\nu_{(CO)}$ 2031 vs, 1981 m, 1952 m, $\nu_{(OCO)}$ 1559 s cm^{-1}. ESI-MS: *m*/*z* = 1266.40 $[M\text{-}CO]^+$. Anal. Calc. for $C_{68}H_{84}O_8P_2Ru_2$: C, 63.16; H, 6.53. Found C, 63.14; H, 6.55%.

$Ru_2(CO)_4\{OOC(CH_2)_{15}CH_3\}_2(C_5H_5N)_2$ (**6a**). Yellow powder, yield 50 mg (43.74%). ^1H NMR (400 MHz, $CDCl_3$): δ = 8.75-8.73 (m, 4H, C_5H_5N), 7.84-7.80 (tt, 2H, C_5H_5N, ^3J = 7.6Hz, ^4J = 1.6 Hz), 7.43-7.40 (ddd, 4H, C_5H_5N, ^3J = 7.6 Hz, ^3J = 4.9 Hz, ^4J = 1.4 Hz), 2.26 (*t*, 4H, CH_2COO, ^3J = 7.2 Hz), 1.26–1.22 (m, 48H, CH_2), 0.88 (*t*, 6H, CH_3, ^3J = 6.8 Hz). $^{13}C\{^1H\}$ NMR (100 MHz, $CDCl_3$): δ = 204.12 (CO), 186.84 (COO), 151.84 (C_5H_5N), 137.21 (C_5H_5N), 124.71 (C_5H_5N), 36.87 (CH_2), 31.89 (CH_2), 29.69 (CH_2), 29.63 (CH_2), 26.59 (CH_2), 26.20 (CH_2), 22.66 (CH_2), 14.36 (CH_3). IR (KBr): $\nu_{(CO)}$ 2022 vs, 1969 m, 1946 m, $\nu_{(OCO)}$ 1567 s cm^{-1}. ESI-MS: *m*/*z* = 955.33 $[M\text{-}2CO]^+$. Anal. Calc. for $C_{48}H_{76}N_2O_8Ru_2$: C, 57.03; H, 7.58; N, 3.02. Found C, 57.01; H, 7.58; N, 3.02%.

$Ru_2(CO)_4\{OOC(CH_2)_{15}CH_3\}_2(PPh_3)_2$ (**6b**). Yellow powder, yield 170 mg (78.92%). ^1H NMR (400 MHz, $CDCl_3$): δ = 7.57-7.35 (m, 30H, CH_{ph}), 1.92 (*t*, 4H, CH_2COO, ^3J = 7.26 Hz), 1.26-0.90 (m, 56H, CH_2), 0.86 (*t*, 6H, CH_3, ^3J = 6.76 Hz). $^{13}C\{^1H\}$ NMR (100 MHz, $CDCl_3$): δ = 205.85(CO), 188.37 (COO), 133.87 (CH_{ph}), 133.81 (CH_{ph}), 133.75 (CH_{ph}), 133.40 (CH_{ph}), 129.51 (CH_{ph}), 128.08 (CH_{ph}), 128.03 (CH_{ph}), 127.99 (CH_{ph}), 37.16 (CH_2), 31.89 (CH_2), 29.63 (CH_2), 29.41 (CH_2), 29.33 (CH_2), 25.74 (CH_2), 22.65 (CH_2), 14.08 (CH_3). $^{31}P\{^1H\}$ NMR (161 MHz, ($CDCl_3$): δ = 14.21 ppm. IR (KBr): $\nu_{(CO)}$ 2022 vs, 1978 m, 1952 m, $\nu_{(OCO)}$ 1567 s cm^{-1}. ESI-MS: *m*/*z* = 1347.93 $[M\text{-}CO]^+$. Anal. Calc. for $C_{74}H_{96}O_8P_2Ru_2$: C, 64.59; H, 7.13. Found C, 64.52; H, 7.02%.

$Ru_2(CO)_4\{OOC(CH_2)_{16}CH_3\}_2(C_5H_5N)_2$ (**7a**). Yellow powder, yield 50 mg (30.80%). ^1H NMR (400 MHz, $CDCl_3$): δ = 8.75-8.73 (m, 4H, C_5H_5N), 7.84-7.80 (m, 2H, C_5H_5N), 7.43-7.40 (m, 4H, C_5H_5N), 2.26 (*t*, 4H, CH_2COO, ^3J = 7.2 Hz), 1.26-1.22 (m, 48H, CH_2), 0.88 (*t*, 6H, CH_3, ^3J = 6.8 Hz). $^{13}C\{^1H\}$ NMR (100 MHz, $CDCl_3$) δ = 186.83 (COO), 151.83 (C_5H_5N), 137.91 (C_5H_5N), 124.19 (C_5H_5N), 36.87 (CH_2), 31.88 (CH_2), 29.68 (CH_2), 29.58 (CH_2), 26.51 (CH_2), 29.19 (CH_2),

TABLE 2. Crystallographic and Structure Refinement Parameters for Complexes **1b**, **2a**, **3a**, **4a**, and **5a**

Parameter	**1b**	**2a**	**3a**	**4a**	**5a**
Chemical formula	$C_{54}H_{56}O_8P_2Ru_2$	$C_{32}H_{44}N_2O_8Ru_2$	$C_{34}H_{48}N_2O_8Ru_2$	$C_{40}H_{60}N_2O_8Ru_2$	$C_{42}H_{64}N_2O_8Ru_2$
Formula weight	1097.07	786.83	814.88	899.04	927.09
Crystal system	Triclinic	Triclinic	Triclinic	Triclinic	Triclinic
Space group	*P*-1 (No. 2)	*P*-1 (No. 2)	*P*-1 (No. 2)	*P*-1 (No. 2)	*P*-1 (No. 2)
Crystal colour and shape	yellow block	yellow block	yellow block	yellow block	yellow block
Crystal size	0.23×0.19×0.16	0.25×0.22×0.18	0.22×0.18×0.15	0.16×0.13×0.11	0.24×0.21×0.16
a, Å	13.2493(13)	10.6836(8)	10.6712(6)	10.6008(14)	10.6356(7)
b, Å	14.4189(14)	11.2916(9)	11.3078(7)	10.9131(17)	11.1666(8)
c, Å	15.0855(15)	15.8511(13)	16.3035(11)	18.886(3)	19.3877(15)
α, deg	106.912(11)	69.609(6)	78.011(5)	94.899(13)	88.198(6)
β, deg	93.503(12)	82.296(6)	84.539(5)	96.721(12)	89.544(6)
γ, deg	109.986(11)	77.458(6)	76.100(4)	101.726(12)	76.654(6)
V, Å^3	2549.6(4)	1746.0(2)	1865.9(2)	2111.1(5)	2239.3(3)
Z	2	2	2	2	2
T, K	173(2)	173(2)	173(2)	173(2)	173(2)
d_c, g·cm^{-3}	1.429	1.497	1.450	1.414	1.375
μ, mm^{-1}	0.707	0.913	0.858	0.765	0.724
Scan range, deg	2.17 < θ < 26.18	1.96 < θ < 29.19	1.89 < θ < 29.19	1.92 < θ < 29.37	1.88 < θ < 29.19
Unique reflections	9374	9140	10080	11378	12099
Reflections used [$I > 2\sigma(I)$]	6441	4338	6410	3606	7893
R_{int}	0.0433	0.1547	0.1053	0.2887	0.1744
Final *R* indices [$I > 2\sigma(I)$]*	0.0370, wR_2 0.0879	0.0795, wR_2 0.1691	0.0529, wR_2 0.0837	0.1064, wR_2 0.2178	0.0680, wR_2 0.1419
R indices (all data)	0.0658, wR_2 0.1115	0.1783, wR_2 0.1388	0.1041, wR_2 0.0943	0.2762, wR_2 0.2874	0.1120, wR_2 0.1574
GOOF	1.010	0.929	0.928	0.862	0.967
Max, Min Δρ, e·Å^{-3}	0.836, –1.314	0.930, –0.839	0.947, –0.857	1.722, –1.187	0.687, –1.219

*Structures were refined on F_0^2: $wR_2 = [\sum[w(F_0^2 - F_c^2)^2]/\sum w(F_0^2)^2]^{1/2}$, where $w^{-1} = [\sum(F_0^2) + (aP)^2 + bP]$ and $P = [\max(F_0^2, 0) + 2F_c^2]/3$.

26.19 (CH_2), 22.64 (CH_2), 14.05 (CH_3). IR (KBr): $\nu_{(CO)}$ 2022 vs, 1969 m, 1945 m, $\nu_{(OCO)}$ 1568 s cm^{-1}. ESI-MS: *m*/*z* = 1012.6 $[M\text{-}CO]^+$. Anal. Calc. for $C_{50}H_{80}N_2O_8Ru_2$: C, 57.89; H, 7.82; N, 2.58. Found C, 57.78; H, 7.76; N, 2.70%.

$Ru_2(CO)_4\{OOC(CH_2)_{16}CH_3\}_2(PPh_3)_2$ (**7b**). Yellow powder, yield 113 mg (34.23%). ^{1}H NMR (400 MHz, $CDCl_3$): δ = 7.56-7.54 (m, 12H, CH_{ph}), 7.52-7.37 (*t*, 18H, CH_{ph}), 1.92 (*t*, 4H, CH_2COO, ^3J = 7.3 Hz), 1.26-0.90 (m, 64H, CH_2), 0.88 (*t*, 6H, CH_3, ^3J = 6.8 Hz). $^{13}C\{^1H\}$ NMR (100 MHz, $CDCl_3$): δ = 205.85 (CO), 188.37 (COO), 133.87 (CH_{ph}), 133.81 (CH_{ph}), 133.75 (CH_{ph}), 133.25 (CH_{ph}), 133.40 (CH_{ph}), 133.25 (CH_{ph}), 37.16 (CH_2), 31.89 (CH_2), 29.63 (CH_2), 29.41 (CH_2), 29.33 (CH_2), 25.74 (CH_2), 22.65 (CH_2), 14.08 (CH_3). $^{31}P\{^1H\}$ NMR (161 MHz, $CDCl_3$): δ = 14.21 ppm. IR (KBr): $\nu_{(CO)}$ 2033 vs, 1982 m, 1950 m, $\nu_{(OCO)}$ 1567 s cm^{-1}. ESI-MS: *m*/*z* = 1348.88 $[M\text{-}2CO]^+$. Anal. Calc. for $C_{76}H_{100}O_8P_2Ru_2$: C, 65.00; H, 7.27. Found C, 64.94; H, 7.17%.

X-ray crystallography. Crystals of complexes **1b**, **2a**, **3a**, **4a**, and **5a** were mounted on a Stoe Image Plate Diffraction system equipped with a ϕ circle goniometer, using MoK_α graphite monochromated radiation (λ = 0.71073 Å) with ϕ range 0-200°. The structures were solved by direct methods using the program SHELXS-97, while the refinement and all further calculations were carried out using SHELXL-97 [9]. The H-atoms were found on Fourier difference map or included

in calculated positions and treated as riding atoms using the SHELXL default parameters. The non-H atoms were refined anisotropically, using weighted full-matrix least-square on F^2. Crystallographic details are summarised in Table 2. Figs. 1 and 2 were drawn with ORTEP [10].

SUPPLEMENTARY DATA

CCDC 765243 (**1b**), 765244 (**2a**), 765245 (**3a**), 765246 (**4a**), and 765247 (**5a**) contain the supplementary crystallographic data for this paper. These data can be obtained free of charge from The Cambridge Crystallographic Data Centre via www.ccdc.cam.ac.uk/data_request/cif.

JJP is grateful to the Swiss Commission of Fellowship for financial support. A generous loan of ruthenium chloride hydrate from the Johnson Matthey Technology Centre is gratefully acknowledged.

REFERENCES

1. G. R. Crooks, B. F. G. Johnson, J. Lewis, et al., *J. Chem. Soc A*, 2761 (1969).
2. H. Schumann, J. Opitz, and J. Pickardt, *J. Organomet. Chem*., **128**, 253 (1977).
3. B. Therrien and G. Süss-Fink, *Coord. Chem. Rev*., **253**, 2639 and refs. Therein (2009).
4. M. Auzias, J. Mattsson, B. Therrien, and G. Süss-Fink, *Z. Anorg. Allg. Chem*., **635**, 115 (2009).
5. M. Auzias, B. Therrien, and G. Süss-Fink, *Inorg. Chim. Acta*, **359**, 3412 (2006).
6. M. Auzias, B. Therrien, G. Labat, et al., *Inorg. Chim. Acta*, **359**, 1012 (2006).
7. S. Tsuzuki, K. Honda, T. Uchimura, et al., *J. Am. Chem. Soc*., **124**, 104 (2002).
8. M. I. Bruce, C. M. Jensen, and N. L. Jones, *Inorg. Synth*., **26**, 259 (1989).
9. G. M. Sheldrick, *Acta Crystallogr*., **A64**, 112 (2008).
10. L. J. Farrugia, *J. Appl. Crystallogr*., **30**, 565 (1997).